Element-selective analysis of ultrafast demagnetization in Co/Pt multilayers exhibiting large perpendicular magnetic anisotropy

M. Hennes, G. Lambert, V. Chardonnet, R. Delaunay, G. Chiuzbăian, E. Jal, B. Vodungbo

Element-Selective Analysis of Ultrafast Demagnetization in Co/Pt Multilayers Exhibiting Large Perpendicular Magnetic Anisotropy

M. Hennes,[1, a)] G. Lambert,[2] V. Chardonnet,[1] R. Delaunay,[1] G. S. Chiuzbăian,[1] E. Jal,[1] and B. Vodungbo[1, a)]
[1)]*Sorbonne Université, CNRS, Laboratoire de Chimie Physique—Matière et Rayonnement, LCPMR, 75005 Paris, France*[b)]
[2)]*Laboratoire d'Optique Appliquée, ENSTA ParisTech, CNRS, École Polytechnique, Institut Polytechnique de Paris, 828 Bd des Maréchaux, 91702 Palaiseau, France*

(Dated: 8 February 2022)

We use time-resolved resonant magnetic scattering experiments to investigate the laser induced demagnetization of Co/Pt multilayers with large perpendicular magnetic anisotropy (PMA). Our pump-probe approach, which relies on extreme ultraviolet (XUV) pulses obtained via high-harmonic generation (HHG), allows to monitor the temporal evolution of the system in an element-selective fashion and thus to disentangle the contributions from permanent and proximity-induced magnetic moments. By analyzing the data gathered at the Co $M_{2,3}$ and Pt O_3 edges, we are able to show that, after femtosecond laser irradiation, both components display a very similar loss of magnetic order, with almost identical demagnetization amplitudes and characteristic times, but a small delay (10 -20 fs) of the Pt magnetization quenching with respect to Co. Comparing our experiments with literature results therefore suggests that in these 3d-5d multilayers and alloys, the different constituents remain strongly coupled after optical excitation, no matter whether the thin films possess a preferred in-plane or out-of-plane easy magnetization direction.

Multilayer thin films and alloys combining 3d and 4d or 5d metals such as Co/Pt, Fe/Pt or Co/Pd have been analyzed for decades because of their remarkable magnetic properties, in particular, their capacity to display a large perpendicular anisotropy[1–4]. Recently, these material systems have generated great interest in the field of ultrafast magnetism: They turned out to be well-suited tools to study the flow of ultrafast spin and charge currents[5–8], to analyze magnetic domain modifications following femtosecond laser irradiation[9,10], or all-optical switching phenomena[11–13] that might pave the way for the development of future spintronic and data storage applications.

Surprisingly, the sublattice-specific magnetization dynamics in these systems are still incompletely understood. While the appearence of proximity-induced magnetic moments in bulk paramagnetic 4d and 5d components is well-established[14–16], it is not clear how the ferromagnetic and the induced moments behave when the system is optically excited on ultrashort timescales. In fact, conflicting results have been published in recent years, raising questions about the impact of the sample properties on the ultrafast magnetic response. Willems *et al.*, performed magnetic circular dichroism (MCD) experiments on thin magnetic Pt/Co/Pt sandwiches in the extreme ultraviolet (XUV) spectral range (at the $M_{2,3}$ edges of Co and O edges of Pt) and concluded that Co and Pt demagnetize simultaneously on femtosecond time scales[17]. In a similar study Hofher *et al.* scrutinized randomly alloyed Fe-Pt thin films using transverse magneto-optical Kerr effect (MOKE) measurements based on high harmonic generation and observed an identical normalized transient de- and remagnetization for Fe and Pt[18]. Vaskivskyi *et al.* employed the same technique to analyze chemically disordered Co-Pt films: the higher accuracy of their measurements allowed to unravel slight differences in the demagnetization amplitudes and rates, but overall, the sublattice-specific magnetization dynamics were found to be very similar[19].

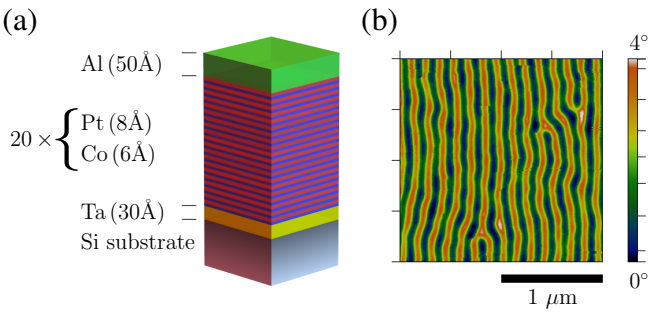

FIG. 1. Co/Pt thin film structure and stripe domain formation. a) Schematic of the multilayers employed in the present study. b) Magnetic force microscopy (MFM) imaging (phase signal) demonstrates the formation of nanometer-sized magnetic domains.

In contrast to these findings – all of them obtained on samples displaying a characteristic in-plane magnetization – experiments performed on thin films with pronounced out-of-plane anisotropy hint at very different dynamics in the two magnetic sub-systems. In a time-resolved MCD study performed using hard x-ray pulses at the Pt L edge, Yamamoto *et al.* observed a slow demagnetization of the Pt moment in $L1_0$-ordered Fe-Pt thin films. With the complementary use of tr-MOKE measurements, they demonstrated that this decay time differed by more than a factor of six, when compared to the overall, Fe-dominated magnetization[20]. In a follow-up study based on polar X-MOKE measurements, similar results were obtained on Co/Pt multilayers. Again, Co was found to demagnetize much faster[21].

Taken together, these experiments suggest that the mag-

[a)]Electronic mail: Authors to whom correspondence should be addressed: marcel.hennes@sorbonne-universite.fr and boris.vodungbo@sorbonne-universite.fr
[b)]M. Hennes currently at: Sorbonne Université, CNRS-UMR 7588, Institut des NanoSciences de Paris, INSP, 75005 Paris, France

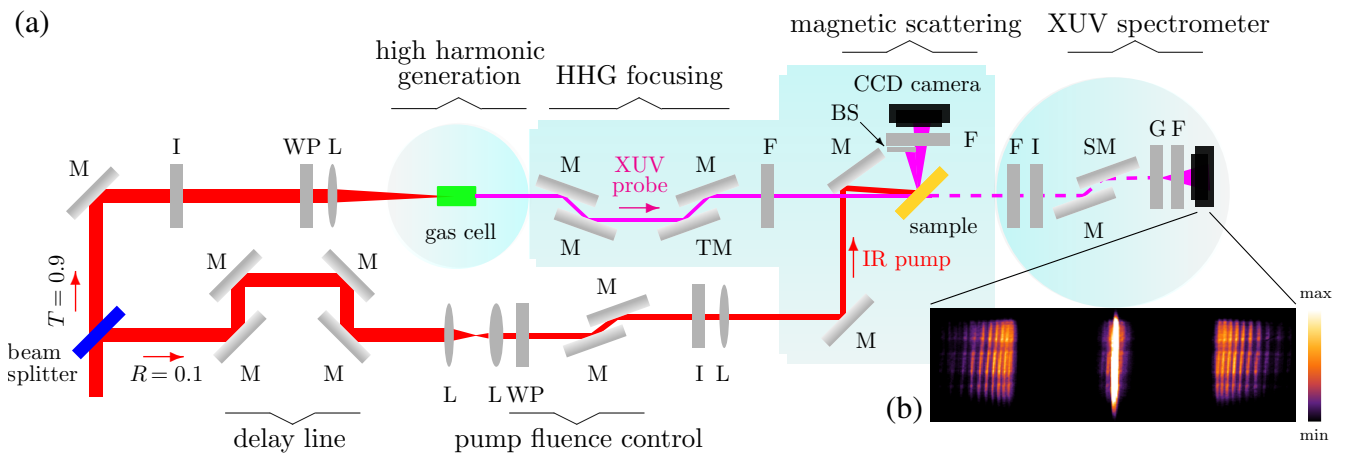

FIG. 2. Pump-probe time-resolved XUV resonant magnetic scattering setup. a) Details of the experiment. M: flat mirror, TM: toroidal mirror, SM: spherical mirror, I: iris, L: lens, WP: $\lambda/2$ wave plate, BS: beam stop, F: Al filter, G: grating. The pressure in the HHG chamber (light blue) is kept below $p < 10^{-4}$ mbar. b) Spectrometer CCD snapshot.

netic anisotropy could have an impact on the demagnetization processes. However, it must also be emphasized that the aforementioned studies did not all rely on the use of the same probing wavelengths. To what extent this can affect the apparent ultrafast response of the system remains to be fully elucidated[22,23]. In the present letter, we therefore disentangle these effects by studying the laser-induced demagnetization of Co and Pt layers at the $M_{2,3}$ and O_3 edges, using samples with strong PMA. Our results clearly demonstrate that both elements display an almost identical de- and remagnetization behavior. This underpins that the specific anisotropy of the system, i.e., out-of-plane (OP) or in-plane (IP), has only a minor influence on the ultrafast magnetization dynamics.

All samples analyzed in the present study consist of magnetic multilayers with nominal composition $[Co(0.6\,nm)/Pt(0.8\,nm)]_{20}$. The films were sputter-deposited on Si substrates, using a 3 nm thin Ta adhesion layer, as well as a 5 nm Al capping to prevent oxidation. The nominal structure of the films is depicted in Fig. 1a. As demonstrated in earlier work, such thin films display a large OP anisotropy, which results in the creation of nanometer-sized domains that reduce the overall magnetic free energy of the system. The PMA was checked using static MOKE measurements (Supplementary Material S1) while the presence of domains was evidenced using magnetic force microscopy (Park NX20). As shown in Fig. 1b, the domains can be aligned using an appropriate in-plane demagnetization procedure. A characteristic stripe periodicity $w = 138 \pm 3$ nm was extracted from the phase signal, and found to be in good agreement with other studies employing similar multilayers[24].

To unravel the demagnetization of the thin films following ultrafast optical excitation, we set up a pump-probe XUV magnetic scattering experiment ("salle corail" at the Laboratoire d'Optique Appliquée) based on the use of a 5 kHz infrared laser system (Coherent laser Elite duo) with wavelength $\lambda \simeq 800$ nm, typical pulse duration of about 30 fs and energy $E = 2.5$ mJ. As shown in Fig.2, a beam splitter was used to separate the incoming beam into pump and probe pulses possessing 10% (reflectivity) and 90% (transmission) of the initial energy, respectively. The probe beam is then p-polarized with the help of a $\lambda/2$ waveplate, and focused into a 3 cm long, cylindrical gas cell filled with neon (or argon) for HHG. Note that by carefully adjusting the source parameters, such as the focal position in the gas cell, the iris aperture, the laser chirp, and the gas pressure, it is possible to optimize the generation efficiency in the targeted spectral range for our magnetic spectroscopy studies[25]. The generated probe beam is reflected by a combination of three flat SiO_2 mirrors placed in grazing incidence geometry and a gold-covered toroidal mirror used to focus the XUV radiation onto the sample (located at a distance of 1.5 m). A 150-nm-thick aluminum filter can be placed into the beam path to remove the residual IR radiation. The magnetic thin films are mounted on a motorized sample holder which allows to remove the magnetic multilayers from the beam axis. In that configuration, the HHG spectrum can be analyzed thanks to a precisely calibrated in-line spectrometer, composed of a second aluminum filter, an iris, a gold mesh (1000 lines per mm grating), and a grazing incidence spherical mirror that focuses the resulting XUV pulses onto a CCD camera (Princeton PI-MTE). Moving the sample into the beam path allows to record magnetic diffraction patterns on a second CCD camera (Princeton Pixis).

To study the magnetic dynamics of our sample, a motorized optical delay line was installed in the pump beam path and supplemented by different optical and mechanical components: a telescope to reduce the size of the IR pump beam by a factor of 5, an iris adjusted to 2-3 mm aperture and a lens ($f = 1$ m). This allowed to obtain a homogeneous irradiation on the sample and a pump spot sufficiently large to exceed the size of the HHG probe beam. Note that the intensity of the excitation pulses was adjusted with the help of a half wave plate placed before a set of two flat mirrors, positioned such as to favor the reflection of the s-polarization component.

While a series of static and dynamic resonant magnetic

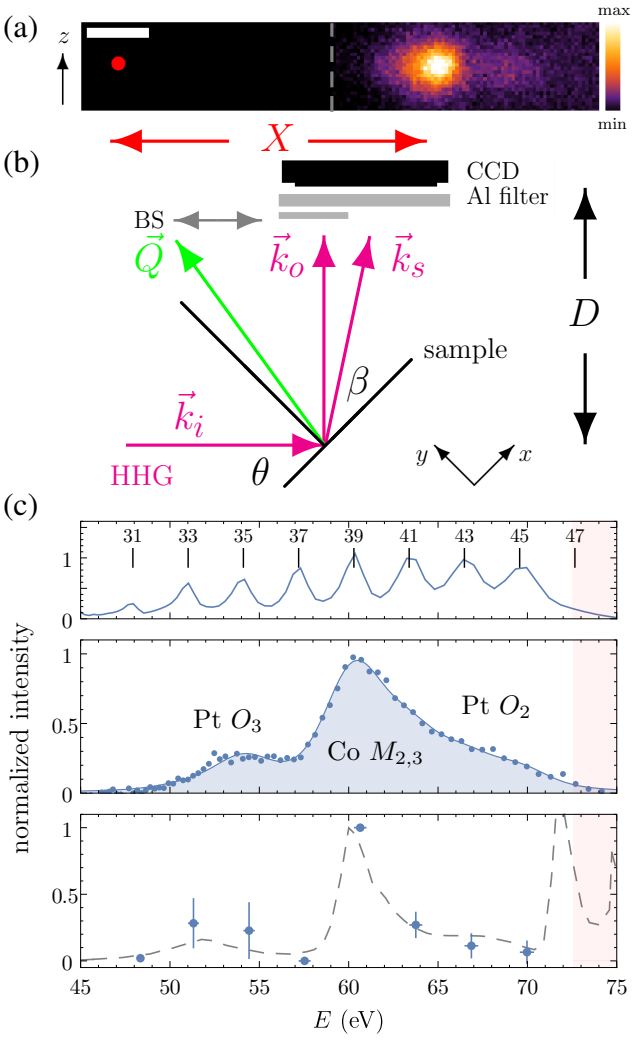

FIG. 3. Resonant magnetic scattering in reflection geometry. a) Exemplary scattering intensity recorded on the CCD (8×8 binning). The edge of the beam-stop (BS) is highlighted by the gray dashed line. Moving the BS allows to determine the position of the specular reflection (red dot) and to calculate X. Scale bar: 2 mm. b) Schematic of the scattering geometry used in the present study, $\vec{k}_i$: wave vector of the incoming HHG pulse, $\vec{k}_o$: wave vector of the reflected HHG pulse, $\vec{k}_s$: wave vector of the diffracted beam. BS: beam stop. c) HHG generation in Ne: intensities and calculated maxima positions (top). Note that the broad peaks (and mutual overlapping) observed here result from a rather poor spectrometer resolution, and do not reflect the true harmonics widths. Exemplary CCD intensity integrated along z after pixel to energy conversion. Blue filling: Voigt curve fits (middle). Extracted averaged Voigt amplitudes (blue dots) obtained by analyzing different samples and angles θ. Comparison with literature data (dashed gray)[24]. The Al filter strongly reduces the signal above 72.55 eV (red filling).

scattering studies have been presented in the last years, most of them were based on the analysis of the HHG intensities transmitted through the sample[9,10,24,26–29]. In contrast, the present experiments were performed in reflection geometry. Just as in the transmission case, the multilayer acts as a magnetic grating for the incoming HHG beam, giving rise to magnetic diffraction spots that provide detailed information on the magnetization and spin structure of the sample[30].

A static CCD camera picture demonstrating the presence of magnetic scattering peaks is shown in Fig. 3a. Fig. 3b provides a detailed description of the scattering geometry used in our work. Constructive interference, i.e., a magnetic diffraction peak is observed when

$$\vec{Q}\cdot\vec{e}_x = 2\pi/w \tag{1}$$

Here, $\vec{Q}$ represents the scattering vector $\vec{Q}=\vec{k}_s-\vec{k}_i$, i.e., the difference between the incoming and scattered wave vectors $\vec{k}_i$ and $\vec{k}_s$, while $\vec{e}_x$ is the unit vector in x direction, as shown in Fig. 3b. This allows to write the scattering angle β (the angle between the scattering wavevector $\vec{k}_s$ and the surface of the sample) as a function of the wavelength λ, the incidence angle θ (the angle between the incident wavevector $\vec{k}_i$ and the surface of the sample) and the periodicity w of the magnetic domains:

$$\beta = \arccos(\lambda/w+\cos(\theta)) \tag{2}$$

It is then straightforward to link β to the camera position using the sine rule (note that the camera is always placed perpendicularly to the incoming HHG beam):

$$\frac{X}{\sin(\theta-\beta)} = \frac{D}{\sin(\theta+\beta)} \tag{3}$$

Here, X denotes the position of the scattering peak on the camera, with respect to the specular beam, while D describes the distance between the surface of the sample and the CCD, as depicted in Fig. 3a and Fig. 3b ($D\simeq 50$ mm, depending on the specific setup geometry). With a combination of eq. 2 and eq. 3 one can thus translate each camera pixel into an average wavelength (given a sufficiently narrow domain size distribution).

As shown in Fig. 3a, the main magnetic peak, resulting from resonant scattering at the Co $M_{2,3}$ edges, exhibits a substructure: a second faint satellite maximum can be identified at larger X values. This becomes even more apparent when projecting the data along z, the direction perpendicular to the plane of incidence, as shown in Fig. 3c. Note that the broadening of the scattering peaks results from the domain size distribution, while our probing harmonics have a relative energy resolution of around 1%[31]. To analyze these features in a more quantitative fashion, the spectra were fitted using Voigt curves centered at the harmonics maxima (Fig.3c). The extracted amplitudes were subsequently normalized with the harmonics intensities (deduced from the spectrometer data) and eventually compared with earlier resonant magnetic scattering experiments performed at the free electron laser Fermi on a similar sample[24]. As shown in Fig. 3c (bottom), good agreement with the measurements of Willems *et al.* is observed. This allows to draw three important conclusions: a) in

our experiments, the aforementioned second weaker peak results from scattering of photons with wavelengths corresponding to the harmonics H33 and H35, probing the Pt O_3 edge, b) the asymmetry of the Co peak hints at the presence of a second resonance between 65 eV and 70 eV, which can be attributed to the Pt O_2 edge, and finally, c) the Pt $N_{6,7}$ edges (above 70 eV) do not yield any measurable signal in our work due to the presence of the Al filter cutoff at 72.55 eV.

With this quantitative description of the static data at hand, it is now possible to obtain an element-selective view on the demagnetization dynamics of the system, by analyzing the temporal evolution of the distinct magnetic diffraction spots following optical excitation of the multilayer. Therefore, for each pump-probe delay, we compared the intensities integrated over the Co $M_{2,3}$ and Pt O_3 peaks[19,32]. As $M \propto \sqrt{I}$, these data thus provide direct insight into the temporal evolution of the Co and induced Pt moment. Note that special care was taken to subtract the background signal, a non-trivial task which has a large impact on the resulting data, considering the very different signal to noise ratios (SNR) of the Co and Pt scattering maxima (Supplementary Material S2).

Fig.4a shows time-resolved resonant magnetic scattering measurements performed using different IR pump fluences. In all cases, the measured intensity is found to drop rapidly during the first 200 fs after excitation of the system, the characteristic signature of optically induced ultrafast demagnetization[33]. On longer timescales, typically several tens to hundreds of ps, the magnetization recovers as a consequence of energy transport out of the magnetic thin film. As can clearly be seen in these measurements, data gathered at the Co and Pt edges result in the same time traces, which is the central result of the present letter: irrespective of the employed fluence, we observe that the Co and Pt layers display an almost identical de- and remagnetization behavior. Note that this holds true for all incidence angles employed in our work ($37^\circ < 90-\theta < 45^\circ$).

To gain further quantitative insight into the initial femtosecond dynamics of the Co/Pt multilayers, we fitted the transient magnetic behavior using a double exponential function convoluted with a Gaussian curve to account for the finite width of the excitation pulse[21]:

$$\frac{M(t)}{M_0} = G(\sigma,t) * \left(1 - A(1-e^{-t/\tau_M}) \cdot (a + (1-a)e^{-t/\tau_{rec}})H(t)\right) \quad (4)$$

Here, τ_M and τ_{rec} are the characteristic de- and remagnetization time constants, while the parameters A and a determine the amplitude of the quenching and subsequent recovery. $H(t)$ is the Heaviside function. Note that t_0, i.e., the onset of the demagnetization is set to zero in the above equation. Fig. 4b presents exemplary data gathered at the Co $M_{2,3}$ and Pt O_3 edges for two different pump fluences Φ. Choosing pulse widths $35\,\text{fs} < \sigma < 45\,\text{fs}$ we obtain typical time constants $\tau_M(\text{Co}) = 101 \pm 22\,\text{fs}$ and $\tau_M(\text{Pt}) = 94 \pm 26\,\text{fs}$ which are in rather good agreement with recent results gathered on Co-Pt alloys[19]. However, in contrast to what has been observed there, we do not see any systematic difference between $\tau_M(\text{Co})$ and $\tau_M(\text{Pt})$. We also emphasize that we do not find any significant variation of the demagnetization time constants with excitation fluence[19].

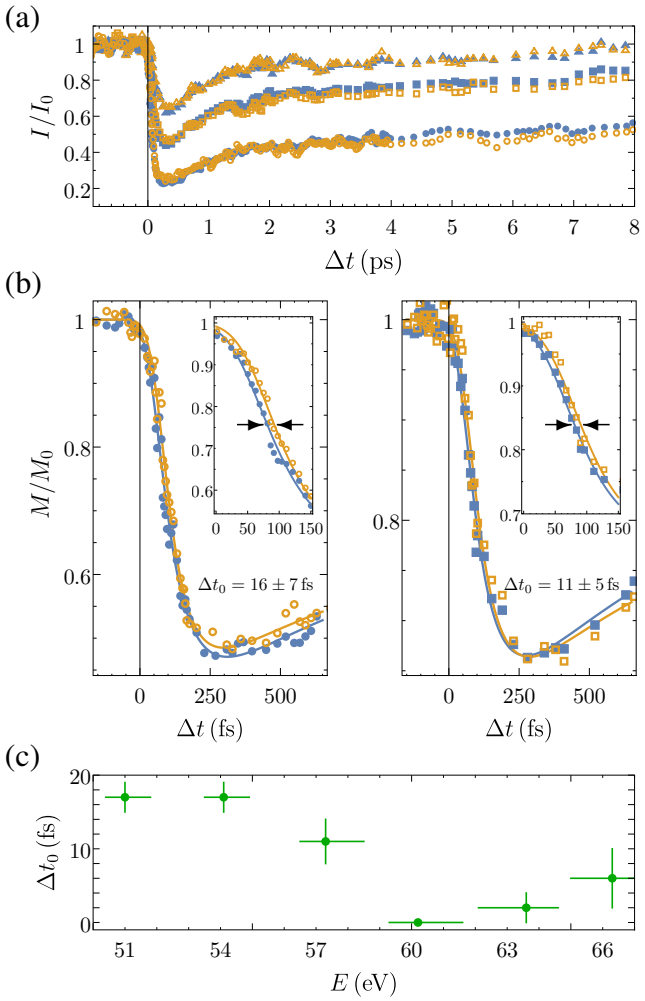

FIG. 4. Element-selective analysis of laser-induced ultrafast demagnetization. a) Scattered intensities integrated at the Co $M_{2,3}$ and Pt O_3 edges (filled blue and orange open symbols, respectively) as a function of the pump-probe delay Δt shown for increasing IR pump fluences $\Phi = 10$ mJ/cm^2 (triangles), $\Phi = 19$ mJ/cm^2 (squares), and $\Phi = 24$ mJ/cm^2 (circles). b) Transient demagnetization and fits to the data (using a double exponential function) shown for two different pump fluences (same color code). Inset: magnified view on the first Δt =150 fs. In both cases, a small temporal lag Δt_0 between the onset of the Co and Pt quenching is observed. c) Δt_0 (obtained by fitting a single exponential convoluted with a Gaussian to the initial magnetization decay) using small probing energy windows centered around the harmonics (H33 – H43).

Rather surprisingly, our fits indicate that the Pt demagnetization is delayed with respect to Co, as can be seen in the insets of Fig.4b. The observed temporal lag $\Delta t_0 = t_0(\text{Pt}) - t_0(\text{Co})$ is small, typically in the range 10-20 fs but we observe it in all samples that were analyzed and independently of the excitation fluence Φ. To cross-check this result and understand, whether it might depend on the different signal to noise ratios of the intensities measured at the two different edges,

or the specific geometry used in our experiments, additional measurements were performed by changing the inert gas in the cylindrical HHG cell. Using Ar instead of Ne allows to probe the system at lower energies, with significant XUV intensity generated in the range $37\,\mathrm{eV} < E_{\mathrm{HHG}} < 57\,\mathrm{eV}$, providing a more detailed view on the Pt O_3 edge (Supplementary Material S3). By fitting these data, we find characteristic demagnetization time constants in good agreement with our results in Ne, but we do not see any indication for a shift when using different integration windows (Supplementary Material S4). This is further confirmed by integrating specifically over each of the harmonics, i.e., analyzing the response of the system using H33 to H39, separately, when working with Ne. To avoid any shortcomings linked to poor SNR, we smoothed the time traces using a moving average filter and fitted exclusively the first 300 fs of the quenching process with a single exponential decay, convoluted with a Gaussian function. As can be seen in Fig. 4c, the characteristic shifts are approximately constant at each edge, but differ significantly between Co and Pt. In contrast, the τ_{M} values are found to be approximately equal for all 6 harmonics that were scrutinized (data not shown).

This unexpected behavior is reminiscent of observations made during ultrafast demagnetization of $Fe_{0.2}Ni_{0.8}$ alloys, where a similar delay of about 18 fs was observed and claimed to reflect the characteristic exchange interaction timescale of the system[34]. While these results have been controversially discussed, recent TMOKE and XMCD measurements advocate the existence of a temporal lag as large as 40-50 fs when quenching the magnetization of the two permalloy components with ultrafast optical pulses[35]. Considering the strikingly similar timescales, it is thus tempting to conclude that comparable mechanisms are at work here. At the same time, it appears puzzling that, with regard to the large amount of literature devoted to element specific magnetization dynamics in 3d-4d and 3d-5d multicomponent systems, this effect has not yet been observed. In the present case, two different aspects must further be taken into closer consideration. First, it is necessary to emphasize that we are also sensitive to the size of the domains and their distribution, which might impact the resulting analyzed intensities. Note however that our experiments do not yield any indication for such modifications. If complex changes of the overall spin structure of the sample were to impact the results, we would also expect a fluence dependence of the data, which is not observed here. Secondly, as recently put forward, electron occupancy changes close to the Fermi level can have a major impact on the observed time traces when using probe beams with small bandwidth[22,23]. Similar effects could play a role in the present experiments and therefore deserve further investigation.

Thus, to conclude, the present work provides evidence for a similar femtosecond response of the ferromagnetic and induced moments in Co/Pt multilayer thin films exhibiting strong PMA, when these are excited by IR pulses on ultrashort timescales. This suggests that the discrepancy between the Co and Pt magnetization dynamics discussed at the beginning of this letter might be attributed to the edges that are put under scrutiny, which raises fundamental questions with regard to data interpretation in femtomagnetism experiments and requires further systematic studies. The delayed response Δt_0, observed in our work, also needs additional efforts to be correctly interpreted. HHG sources with even higher temporal resolution could be useful tools to provide a more quantitative view on this phenomenon. Coupling such experiments with theoretical considerations might bring additional insight into the mechanisms underlying ultrafast magnetization quenching on timescales $\Delta t \ll 100\,\mathrm{fs}$, ultimately paving the way for the design of novel, technologically promising multicomponent nanostructures.

SUPPLEMENTARY MATERIAL

Static MOKE measurements, details concerning the background subtraction routine, a comparison between HHG in Ne and Ar, as well as time traces obtained using the two different gases for HHG are provided in the supplementary material.

ACKNOWLEDGMENTS

The authors are grateful for financial support received from the CNRS-MOMENTUM, and Émergence - Sorbonne Université MADAM programs and would like to thank H. Cruguel for technical support with the AFM measurements.

[1] P. F. Carcia, A. D. Meinhaldt, and A. Suna, "Perpendicular magnetic anisotropy in Pd/Co thin film layered structures," Applied Physics Letters **47**, 178–180 (1985).

[2] P. F. Carcia, "Perpendicular magnetic anisotropy in Pd/Co and Pt/Co thin-film layered structures," Journal of Applied Physics **63**, 5066–5073 (1988).

[3] B. N. Engel, C. D. England, R. A. Van Leeuwen, M. H. Wiedmann, and C. M. Falco, "Interface magnetic anisotropy in epitaxial superlattices," Phys. Rev. Lett. **67**, 1910–1913 (1991).

[4] M. T. Johnson, P. J. H. Bloemen, F. J. A. den Broeder, and J. J. de Vries, "Magnetic anisotropy in metallic multilayers," Reports on Progress in Physics **59**, 1409–1458 (1996).

[5] G. Malinowski, F. Dalla Longa, J. H. H. Rietjens, P. V. Paluskar, R. Huijink, H. J. M. Swagten, and B. Koopmans, "Control of speed and efficiency of ultrafast demagnetization by direct transfer of spin angular momentum," Nature Physics **4**, 855–858 (2008).

[6] N. Moisan, G. Malinowski, J. Mauchain, M. Hehn, B. Vodungbo, J. Lüning, S. Mangin, E. E. Fullerton, and A. Thiaville, "Investigating the role of superdiffusive currents in laser induced demagnetization of ferromagnets with nanoscale magnetic domains," Scientific Reports **4**, 4658 (2014).

[7] B. Vodungbo, B. Tudu, J. Perron, R. Delaunay, L. Müller, M. H. Berntsen, G. Grübel, G. Malinowski, C. Weier, J. Gautier, G. Lambert, P. Zeitoun, C. Gutt, E. Jal, A. H. Reid, P. W. Granitzka, N. Jaouen, G. L. Dakovski, S. Moeller, M. P. Minitti, A. Mitra, S. Carron, B. Pfau, C. von Korff Schmising, M. Schneider, S. Eisebitt, and J. Lüning, "Indirect excitation of ultrafast demagnetization," Scientific Reports **6**, 18970 (2016).

[8] T. J. Huisman, R. V. Mikhaylovskiy, J. D. Costa, F. Freimuth, E. Paz, J. Ventura, P. P. Freitas, S. Blügel, Y. Mokrousov, T. Rasing, and A. V. Kimel, "Femtosecond control of electric currents in metallic ferromagnetic heterostructures," Nature Nanotechnology **11**, 455–458 (2016).

[9] B. Vodungbo, J. Gautier, G. Lambert, A. B. Sardinha, M. Lozano, S. Sebban, M. Ducousso, W. Boutu, K. Li, B. Tudu, M. Tortarolo, R. Hawaldar, R. Delaunay, V. López-Flores, J. Arabski, C. Boeglin, H. Merdji, P. Zeitoun, and J. Lüning, "Laser-induced ultrafast demagnetization in the presence of a nanoscale magnetic domain network," Nature Communications **3**, 999 (2012).

[10] B. Pfau, S. Schaffert, L. Müller, C. Gutt, A. Al-Shemmary, F. Büttner, R. Delaunay, S. Düsterer, S. Flewett, R. Frömter, J. Geilhufe, E. Guehrs,

C. M. Günther, R. Hawaldar, M. Hille, N. Jaouen, A. Kobs, K. Li, J. Mohanty, H. Redlin, W. F. Schlotter, D. Stickler, R. Treusch, B. Vodungbo, M. Kläui, H. P. Oepen, J. Lüning, G. Grübel, and S. Eisebitt, "Ultrafast optical demagnetization manipulates nanoscale spin structure in domain walls," Nature Communications **3**, 1100 (2012).

[11] C.-H. Lambert, S. Mangin, B. S. D. C. S. Varaprasad, Y. K. Takahashi, M. Hehn, M. Cinchetti, G. Malinowski, K. Hono, Y. Fainman, M. Aeschlimann, and E. E. Fullerton, "All-optical control of ferromagnetic thin films and nanostructures," Science **345**, 1337–1340 (2014).

[12] R. Medapalli, D. Afanasiev, D. K. Kim, Y. Quessab, S. Manna, S. A. Montoya, A. Kirilyuk, T. Rasing, A. V. Kimel, and E. E. Fullerton, "Multiscale dynamics of helicity-dependent all-optical magnetization reversal in ferromagnetic Co/Pt multilayers," Phys. Rev. B **96**, 224421 (2017).

[13] G. Kichin, M. Hehn, J. Gorchon, G. Malinowski, J. Hohlfeld, and S. Mangin, "From multiple- to single-pulse all-optical helicity-dependent switching in ferromagnetic Co/Pt multilayers," Phys. Rev. Applied **12**, 024019 (2019).

[14] G. Schütz, S. Stähler, M. Knülle, P. Fischer, S. Parkin, and H. Ebert, "Distribution of magnetic moments in Co/Pt and Co/Pt/Ir/Pt multilayers detected by magnetic x-ray absorption," Journal of Applied Physics **73**, 6430–6432 (1993).

[15] F. Wilhelm, P. Poulopoulos, G. Ceballos, H. Wende, K. Baberschke, P. Srivastava, D. Benea, H. Ebert, M. Angelakeris, N. K. Flevaris, D. Niarchos, A. Rogalev, and N. B. Brookes, "Layer-resolved magnetic moments in Ni/Pt multilayers," Phys. Rev. Lett. **85**, 413–416 (2000).

[16] J. Geissler, E. Goering, M. Justen, F. Weigand, G. Schütz, J. Langer, D. Schmitz, H. Maletta, and R. Mattheis, "Pt magnetization profile in a Pt/Co bilayer studied by resonant magnetic x-ray reflectometry," Phys. Rev. B **65**, 020405 (2001).

[17] F. Willems, C. T. L. Smeenk, N. Zhavoronkov, O. Kornilov, I. Radu, M. Schmidbauer, M. Hanke, C. von Korff Schmising, M. J. J. Vrakking, and S. Eisebitt, "Probing ultrafast spin dynamics with high-harmonic magnetic circular dichroism spectroscopy," Phys. Rev. B **92**, 220405 (2015).

[18] M. Hofherr, S. Moretti, J. Shim, S. Häuser, N. Y. Safonova, M. Stiehl, A. Ali, S. Sakshath, J. W. Kim, D. H. Kim, H. J. Kim, J. I. Hong, H. C. Kapteyn, M. M. Murnane, M. Cinchetti, D. Steil, S. Mathias, B. Stadtmüller, M. Albrecht, D. E. Kim, U. Nowak, and M. Aeschlimann, "Induced versus intrinsic magnetic moments in ultrafast magnetization dynamics," Phys. Rev. B **98**, 174419 (2018).

[19] I. Vaskivskyi, R. S. Malik, L. Salemi, D. Turenne, R. Knut, J. Brock, R. Stefanuik, J. Söderström, K. Carva, E. E. Fullerton, P. M. Oppeneer, O. Karis, and H. A. Dürr, "Element-specific magnetization dynamics in Co–Pt alloys induced by strong optical excitation," The Journal of Physical Chemistry C **125**, 11714–11721 (2021).

[20] K. Yamamoto, Y. Kubota, M. Suzuki, Y. Hirata, K. Carva, M. Berritta, K. Takubo, Y. Uemura, R. Fukaya, K. Tanaka, W. Nishimura, T. Ohkochi, T. Katayama, T. Togashi, K. Tamasaku, M. Yabashi, Y. Tanaka, T. Seki, K. Takanashi, P. M. Oppeneer, and H. Wadati, "Ultrafast demagnetization of pt magnetic moment in l10-FePt probed by magnetic circular dichroism at a hard x-ray free electron laser," **21**, 123010 (2019).

[21] K. Yamamoto, S. E. Moussaoui, Y. Hirata, S. Yamamoto, Y. Kubota, S. Owada, M. Yabashi, T. Seki, K. Takanashi, I. Matsuda, and H. Wadati, "Element-selectively tracking ultrafast demagnetization process in Co/Pt multilayer thin films by the resonant magneto-optical kerr effect," Applied Physics Letters **116**, 172406 (2020).

[22] M. Hennes, B. Rösner, V. Chardonnet, G. S. Chiuzbaian, R. Delaunay, F. Döring, V. A. Guzenko, M. Hehn, R. Jarrier, A. Kleibert, and et al., "Time-resolved XUV absorption spectroscopy and magnetic circular dichroism at the Ni $M_{2,3}$-edges," Applied Sciences **11**, 325 (2020).

[23] K. Yao, F. Willems, C. von Korff Schmising, I. Radu, C. Strüber, D. Schick, D. Engel, A. Tsukamoto, J. K. Dewhurst, S. Sharma, and S. Eisebitt, "Distinct spectral response in M-edge magnetic circular dichroism," Phys. Rev. B **102**, 100405 (2020).

[24] F. Willems, C. von Korff Schmising, D. Weder, C. M. Günther, M. Schneider, B. Pfau, S. Meise, E. Guehrs, J. Geilhufe, A. E. D. Merhe, E. Jal, B. Vodungbo, J. Lüning, B. Mahieu, F. Capotondi, E. Pedersoli, D. Gauthier, M. Manfredda, and S. Eisebitt, "Multi-color imaging of magnetic Co/Pt heterostructures," Structural Dynamics **4**, 014301 (2017).

[25] Slight changes to the laser chirp allow to obtain shorter pulses and, consequently, higher intensities. When playing with the iris aperture, a compromise has to be found: On the one hand, reducing the diameter of the latter increases the beam waist, which allows to generate more photons, on the other hand, one has to deal with a decreasing laser intensity at focus in the gas cell.

[26] J. B. Kortright, S.-K. Kim, G. P. Denbeaux, G. Zeltzer, K. Takano, and E. E. Fullerton, "Soft-x-ray small-angle scattering as a sensitive probe of magnetic and charge heterogeneity," Phys. Rev. B **64**, 092401 (2001).

[27] B. Vodungbo, A. B. Sardinha, J. Gautier, G. Lambert, M. Lozano, S. Sebban, E. Meltchakov, F. Delmotte, V. Lopez-Flores, J. Arabski, C. Boeglin, E. Beaurepaire, R. Delaunay, J. Lüning, and P. Zeitoun, "Table-top resonant magnetic scattering with extreme ultraviolet light from high-order harmonic generation," EPL (Europhysics Letters) **94**, 54003 (2011).

[28] V. Cardin, T. Balciunas, K. Légaré, A. Baltuska, H. Ibrahim, E. Jal, B. Vodungbo, N. Jaouen, C. Varin, J. Lüning, and F. m. c. Légaré, "Wavelength scaling of ultrafast demagnetization in Co/Pt multilayers," Phys. Rev. B **101**, 054430 (2020).

[29] M. Hennes, A. Merhe, X. Liu, D. Weder, C. v. K. Schmising, M. Schneider, C. M. Günther, B. Mahieu, G. Malinowski, M. Hehn, D. Lacour, F. Capotondi, E. Pedersoli, I. P. Nikolov, V. Chardonnet, E. Jal, J. Lüning, and B. Vodungbo, "Laser-induced ultrafast demagnetization and perpendicular magnetic anisotropy reduction in a $Co_{88}Tb_{12}$ thin film with stripe domains," Phys. Rev. B **102**, 174437 (2020).

[30] G. van der Laan, "Soft X-ray resonant magnetic scattering of magnetic nanostructures," Comptes Rendus Physique **9**, 570–584 (2008), synchrotron x-rays and condensed matter.

[31] C. Alves, G. Lambert, V. Malka, M. Hehn, G. Malinowski, M. Hennes, V. Chardonnet, E. Jal, J. Lüning, and B. Vodungbo, "Resonant faraday effect using high-order harmonics for the investigation of ultrafast demagnetization," Phys. Rev. B **100**, 144421 (2019).

[32] J. K. Dewhurst, F. Willems, P. Elliott, Q. Z. Li, C. v. K. Schmising, C. Strüber, D. W. Engel, S. Eisebitt, and S. Sharma, "Element specificity of transient extreme ultraviolet magnetic dichroism," Phys. Rev. Lett. **124**, 077203 (2020).

[33] E. Beaurepaire, J.-C. Merle, A. Daunois, and J.-Y. Bigot, "Ultrafast spin dynamics in ferromagnetic nickel," Phys. Rev. Lett. **76**, 4250–4253 (1996).

[34] S. Mathias, C. La-O-Vorakiat, P. Grychtol, P. Granitzka, E. Turgut, J. M. Shaw, R. Adam, H. T. Nembach, M. E. Siemens, S. Eich, C. M. Schneider, T. J. Silva, M. Aeschlimann, M. M. Murnane, and H. C. Kapteyn, "Probing the timescale of the exchange interaction in a ferromagnetic alloy," Proceedings of the National Academy of Sciences **109**, 4792–4797 (2012).

[35] S. Jana, R. Knut, S. Muralidhar, R. S. Malik, R. Stefanuik, J. Åkerman, O. Karis, C. Schüßler-Langeheine, and N. Pontius, "Experimental confirmation of the delayed Ni demagnetization in FeNi alloy," (2021), arXiv:2106.07956 [cond-mat.mtrl-sci].